

## 5 INFLIGHT SCIENCE AND PHOTOGRAPHY

The inflight experiments and photographic tasks conducted during the Apollo 15 mission are discussed in this section. The discussion is concerned primarily with experiment hardware performance and data acquisition operations. In instances where preliminary scientific findings were available at the time of report preparation, they are included, but more complete information on scientific results will be found in reference 2.

The experiments located in the scientific instrument module bay of the service module (**Fig. 5-1**) consisted of a gamma ray spectrometer, an X-ray spectrometer, an alpha-particle spectrometer, a mass spectrometer; and a subsatellite which is the vehicle for a particle shadows/boundary layer experiment, an S-band transponder experiment, and a magnetometer experiment. The subsatellite (**Fig. 5-2**) was launched successfully just prior to transearth injection on August 4 at approximately 2100 G.m.t., and was inserted into a 76.3-by-55.1-mile lunar orbit with an inclination of minus 28.7 degrees. The three subsatellite experiments are expected to acquire data for a period exceeding 1 year. At the time of launch, the moon was in the magnetosheath (transition) region of the earth's magnetosphere (**Fig 5.3**), one of several data collecting regions of scientific interest. All subsatellite experiments are turned off while the battery is being recharged after each tracking revolution. Both the magnetometer and particle shadows/boundary layer experiments are acquiring data on all revolutions except those when the battery is being charged.

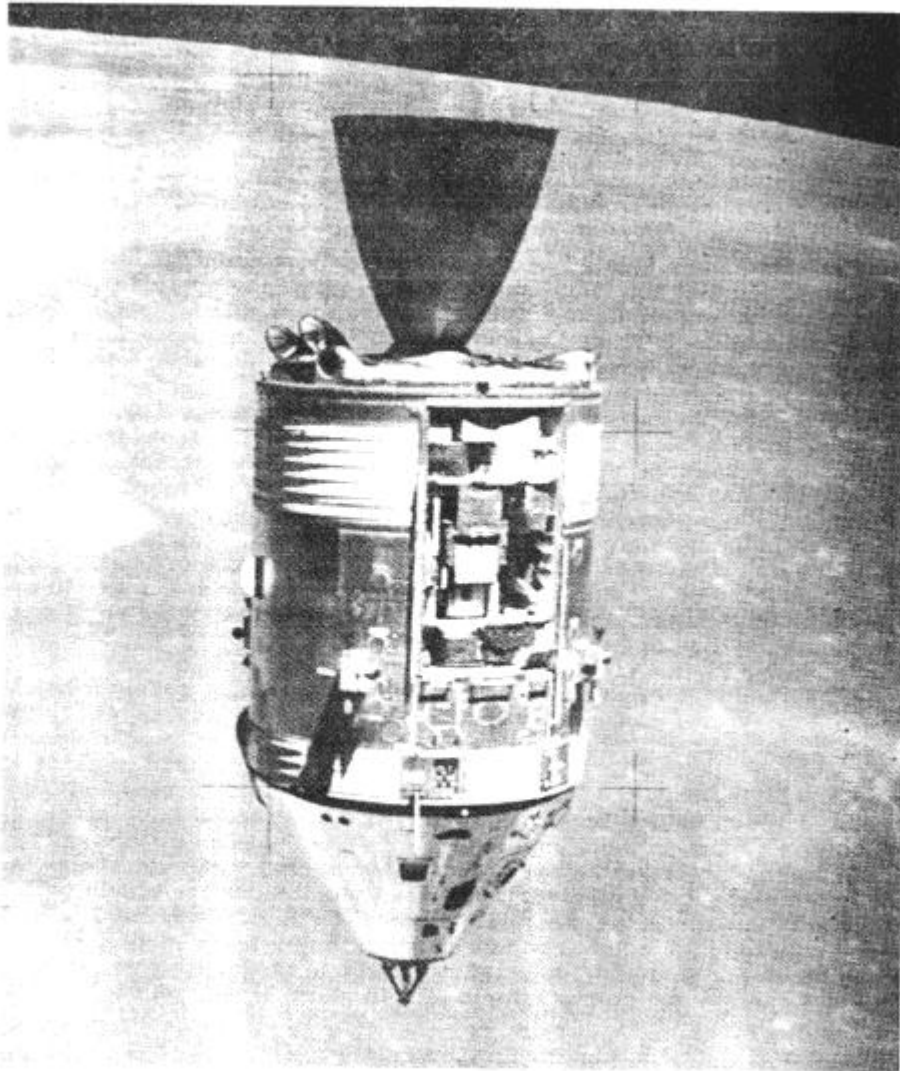


Figure 5-1.- Command and service module as viewed from lunar module during rendezvous.

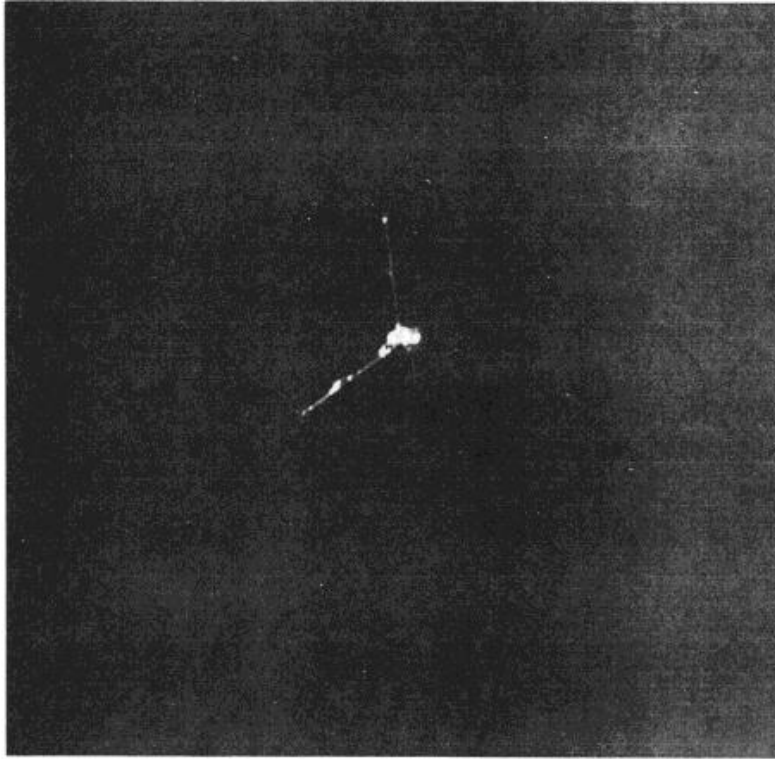


Figure 5-2.- Subsatellite shortly after launch.

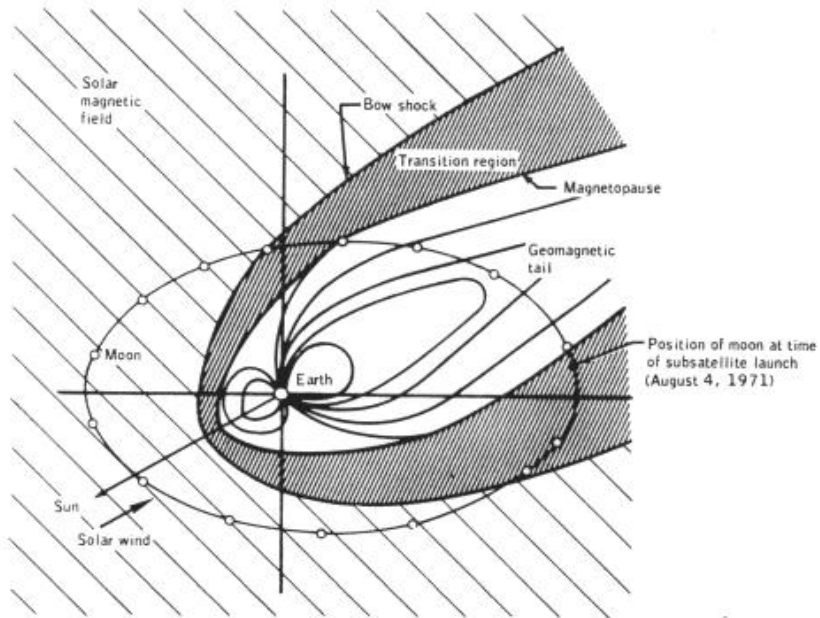


Figure 5-3.- Earth's Magnetosphere

Other inflight experiments consisted of ultraviolet photography of the earth and moon, photography of the Gegenschein from lunar orbit, an S-band transponder experiment using the command and service module and lunar module S-band communication systems, a down-link bistatic radar experiment using both the S-band and VHF communications systems of the command and service module and an Apollo window meteoroid experiment.

Photographic tasks that were designated as detailed objectives rather than experiments are also discussed. They are the service module orbital photography employing the panoramic camera, the mapping camera, and the laser altimeter; and command module photography of lunar surface areas and astronomical subjects. A brief description of the equipment used for these experiments and photographic tasks is given in appendix A.

### **5.1 GAMMA-RAY SPECTROMETER EXPERIMENT**

The gamma-ray spectrometer was operated in lunar orbit for over 90 hours. The instrument was operated in the minimum-background mode for prime data collection approximately 65 percent of the time. The remaining of the time it was operated in various non-minimum-background modes to determine the effects of background radiation sources on the prime data. The instrument was also operated for approximately 50 hours during transearth flight obtaining background data necessary for analysis of the lunar data, and to acquire data from galactic sources.

The instrument as well as the deployment boom performed well throughout the mission. However, two anomalous conditions occurred which affected instrument calibration. First, a downward drift in the linear gain of the photomultiplier or pulse analyzer was detected after the first boom extension (prior to undocking in lunar orbit) when several lines in the spectrum of the Apollo lunar surface experiment package fuel capsule were used for calibrations. The drift decreased in magnitude from an initial rate of 1 percent per hour to 0.4 percent per day and, eventually, reached a fairly stable state. The second anomalous condition was noted about 2-3/4 hours after transearth injection, when spectrum zero shifted eight channels, causing loss of the 0.279-million-electron-volt calibration reference. Commencing at 246:56, the problem disappeared for approximately 25 hours, returning at 271:47 and remaining for the rest of transearth flight. These problems are discussed further in section 14.3.4.

The preliminary data indicates variations in radioactivity as the spacecraft passed over different kinds of terrain. The western mare areas are generally the highest in radioactivity, with the eastern maria being somewhat lower. The highlands are the lowest in activity with a slightly lower level in the far-side highlands. The data further indicate a continuum level comparable to that predicted from Ranger 3 and Luna 10 data. Peaks due to potassium, thorium, oxygen, silicon, and iron have been identified. Detailed analysis is expected to show the presence and distribution of uranium, magnesium, aluminum, and titanium.

### **5.2 X-RAY FLUORESCENCE EXPERIMENT**

All X-ray spectrometer objectives were achieved and no hardware problems were noted. About 90 hours of data were obtained from operation of the instrument in lunar

orbit, and approximately 26 hours of data were acquired while in transearth flight. During this latter period, the instrument was pointed at six preselected locations to acquire data on possible variations in X-ray intensity. Two observations were coordinated with simultaneous ground-based observations. After 276 hours, the instrument was left on to obtain data for use in the search for new sources of X-ray emission and to improve spectral information on known sources.

Near the end of transearth flight, an engineering test was conducted to determine if the gas-filled proportional counters would be damaged by direct impingement of solar X-rays. The experiment continued to operate satisfactorily after the test.

The preliminary data shows that the fluorescent X-ray flux was more intense than predicted; that the concentration of aluminum in the highlands is about 50 percent greater than in the maria; and that the ratio of magnesium-to-aluminum in Mare Smithii and Mare Chrisium is about 50 percent greater than in the highlands between, and to the east and west of, the two maria. Analysis of the X-ray astronomy observations made enroute to the earth has shown that the intensity in X-ray output of Scorpius X-1 and Cygnus X-1 fluctuates with periods of several minutes.

### **5.3 ALPHA-PARTICLE SPECTROMETER EXPERIMENT**

All primary objectives of the alpha-particle experiment were achieved. The spectrometer was operated for approximately 80 hours in lunar orbit to acquire prime data, and approximately 50 hours during transearth coast to acquire background data.

Two of the ten detectors were intermittently noisy. The noise was at a very low rate (approximately 0.5 count per second) with occasional bursts at higher rates. Since the noise was generally restricted to one detector at a time, the loss of data is not expected to have a significant effect on the validity of the analysis.

An engineering test was performed near the end of transearth flight (in conjunction with the test on the X-ray spectrometer). The open experiment covers, which permitted direct sunlight impingement on the instrument, resulted in three of the ten detectors (including the two noisy detectors) showing some evidence of photosensitivity.

The planned coverage of the lunar surface was obtained. The alpha particle spectrometer did not detect any local areas of radon enhancement (An objective of the experiment was to locate craters or fissures by detecting alpha particles emitted by radon isotopes - daughter products of uranium and thorium). The general radon evolution rate of the moon is three orders of magnitude less than that of earth. A refinement of the data, in which summation of counts from successive orbital passes over the same area is made, will be required to make more definitive statements about the lunar distribution of radon isotopes.

### **5.4 MASS SPECTROMETER EXPERIMENT**

Thirty-three hours of prime lunar orbit data were collected with the command and service module minus X axis in the direction of travel, and 7 hours of background data with the command and service module pointed in the opposite direction. During

transearth coast, approximately 48 hours of data were gathered, including waste water dumps, oxygen purges, and boom- retraction tests.

The mass spectrometer boom retract mechanism in the scientific instrument module stalled during five of twelve cycles. Data, supported by the Command Module Pilot's observations during extravehicular activity, confirmed that the boom had retracted to within 1 inch of full retraction.

Each of the five cycles in which the boom did not fully retract was preceded by a period of cold soaking of the boom. In each instance, the boom would retract fully after warm-up. The boom was fully retracted for command module/service module separation. This anomaly is discussed further in section 14.1.6.

The instrument operated well, providing good data. Even though the boom retraction problem resulted in failure to collect prime data during one scheduled period, and real-time scheduling problems prevented instrument operation for another scheduled period, an adequate amount of data was acquired.

The mass spectrometer measured an unexpectedly large amount of gas at orbital altitude around the moon. This amount was an order of magnitude greater than that seen during transearth coast. Many gases were detected, including water vapor, carbon dioxide, and a variety of hydrocarbons. Data obtained during transearth coast indicate that a gaseous contamination cloud existed up to a distance of 4 feet from the command and service module, but contamination was not detected at the maximum extension of the mass spectrometer (24 feet).

### **5.5 PARTICLE SHADOWS /BOUNDARY LAYER EXPERIMENT**

The charged-particle telescope detectors were turned on immediately after subsatellite launch and are operating normally. Proper operation of the proton detection system was indicated when a large flux of protons in the 35 000- to 100 000-electron-volt range were observed near the magnetopause (fig. 5-3). Twenty-four hours after subsatellite launch, the electrostatic analyzer detectors were turned on, and have operated normally with no evidence of high-voltage corona or arcing.

When the moon is not in the earth's geomagnetic tail, the effect of the moon's shadow on the solar wind electrons is clearly detected. The variation in the shadow shape is rather large. With the moon in the earth's tail, a very tenuous plasma is seen. Within the plasma sheet, intensities increase with some flow of plasma from the earth's direction.

### **5.6 SUBSATELLITE MAGNETOMETER EXPERIMENT**

The magnetometer was turned on when telemetry from the subsatellite was acquired, and the instrument has performed satisfactorily. The experiment has operated continuously except for an 18-hour period after the lunar eclipse of August 6, and periods when the power is turned off to enable the batteries to return to full charge.

The magnetometer is returning better-than-expected information in relation to detecting surface anomalies. The principal investigator is carrying out hand calculations on far-side data that indicate excellent repetitive information over the craters Gagarin,

Korolev, and Van de Graaff. While in the solar wind, the magnetometer is mapping the signature of the diamagnetic cavity behind the moon. As the subsatellite crosses the terminator, variations in the solar magnetic field by factors of two to three are detected by the magnetometer. These may be caused by interaction of the solar wind with local magnetic regions near the limb. More careful long-term analysis is required to confirm this preliminary finding.

## **5.7 S-BAND TRANSPONDER EXPERIMENT**

### 5.7.1 Command and Service Module/Lunar Module

Good gravitational profile data along the spacecraft lunar ground tracks were obtained. The anticipated degradation of the data caused by changes in spacecraft position from uncoupled attitude control engine firings was not significant. Indications are that the gross shapes of mascons in Serenitatis, Crisium, and Smythii can be established. This complements the Apollo 14 results on Nectaris. Detailed gravity profiles of the Apennines and Procellarum regions were also obtained.

### 5.7.2 Subsatellite

The initial data contained a high level of noise caused by a wobble about the spin axis. The wobble was inherent in the subsatellite deployment and was subsequently removed by the onboard wobble damper.

The subsatellite S-band transponder is working well, and is being operated every twelfth lunar revolution. The tracking data shows that the perilune variation is following preflight predictions and is expected to confirm the predicted orbital lifetime (greater than 1 year). The subsatellite transponder has shown at least one new mascon in the region of the crater Humboldt on the eastern lunar near side. Repeated overflights of the lunar near side from varying altitudes as the subsatellite orbit decays will be necessary before an accurate gravitational map can be made and large anomalies defined.

## **5.8 DOWN-LINK BISTATIC RADAR OBSERVATIONS OF THE MOON**

The experiment data consists of records of both frequencies (S-band and VHF) during the front-side passes on lunar revolutions 17 and 28. During these dual-frequency periods, signals were bounced off the moon and received at Goldstone (210-ft dish antenna for S-band) and at Stanford University (150-ft dish antenna for VHF). On revolutions 53 through 57 (the crew sleep period), only the VHF frequency was reflected from the moon to the earth.

The experiment results will require considerable data processing. Determination of the bulk dielectric constant and near-surface roughness along the spacecraft track appears possible with the present data. S-band data from revolution 17 are not usable because of incorrect spacecraft attitude. However, VHF data from revolution 17 appear to be of high quality. The attitude error was discovered and corrected in time for revolution 28, and all the data for that revolution are of excellent quality. The VHF experiment conducted during revolutions 53 through 57 provided high quality data. Apollo 15 data may be correlated with data obtained from the Apollo 14 bistatic radar experiment since

the spacecraft groundtracks of Apollo 15 during both S-band/VHF operation and VHF-only operation intersect the Apollo 14 groundtrack during S-band/VHF operation.

### ***5.9 APOLLO WINDOW METEOROID EXPERIMENT***

The command module side and hatch windows were scanned at a magnification of 20X prior to flight to determine the general background of chips, scratches and other defects. Postflight, the windows will again be scanned at 20X (and higher magnifications for areas of interest) to map all visible defects. Possible meteoroid craters will be identified to determine the meteoroid cratering flux of particles responsible for the degradation of glass surfaces exposed to the space environment.

### ***5.10 ULTRAVIOLET PHOTOGRAPHY - EARTH AND MOON***

Ultraviolet photographs were obtained while in earth and lunar orbit, and during translunar and transearth coast. The following table lists the ultraviolet photography sequences performed on Apollo 15. Each sequence consisted of two exposures without the use of a filter and two exposures each with a 2600-angstrom filter, a 3750-angstrom filter, and a 4000- to 6000- angstrom visual-range filter. In addition, some color-film exposures were obtained, as planned, with the visual-range filter. These are noted in the last column of table 5-1. Preliminary examination shows that the exposures were excellent

TABLE 5-I.- ULTRAVIOLET PHOTOGRAPHY

Location of Spacecraft	Subject	Ultraviolet	Color
Earth orbit	Earth limb	8	1
Translunar coast (~ 60 000 n. mi.)	Earth disc	8	1
Translunar coast (~ 60 000 n. mi.)	Moon	8	(a)
Translunar coast (~ 120 000 n. mi.)	Earth disc	8	1
Translunar coast (~ 180 000 n. mi.)	Earth disc	8	1
Lunar orbit	Earth and lunar horizon	8	(a)
Lunar orbit	Earth	8	1
Lunar orbit	Mare areas	<sup>b</sup> 10	(a)
Lunar orbit	Terra area	<sup>b</sup> 10	(a)
Transearth coast (~ 160 000 n. mi.)	Earth disc	8	1
Transearth coast (~ 120 000 n. mi.)	Earth disc	8	1
Transearth coast (~ 60 000 n. mi.)	Earth disc	8	1
Transearth coast (~ 60 000 n. mi.)	Moon/calibration	8	(a)

<sup>a</sup>No color exposures planned.

<sup>b</sup>Four exposures taken with the 4000- to 6000-angstrom filter.

Table 5-I - ULTRAVIOLET PHOTOGRAPHY

### 5.11 GEGENSCHN FROM LUNAR ORBIT

Photography of the Gegenschein and Moulton Point regions from lunar orbit was performed twice, as planned, during revolutions 46 and 60, and at least six exposures were obtained during each sequence. However, the photographs are unusable because incorrect signs were used in premission calculations of spacecraft attitudes. Ground-based photography in support of the inflight photography was performed during the mission at the Haleakala Observatory, Maui, Hawaii, and after the mission at the McDonald Observatory, Fort Davis, Texas.

The camera system used for the Gegendstein experiment and other astronomy tasks performed well. A comparison of preflight and postflight calibration exposures with the faintest brightness observed in the Apollo 15 exposures (of the Milky Way) demonstrates that this camera system is very satisfactory for the Gegendstein experiment, now scheduled for the Apollo 16 mission.

## **5.12 SERVICE MODULE ORBITAL PHOTOGRAPHY**

### **5.12.1 Panoramic Camera**

The panoramic camera was carried on Apollo 15 to obtain high-resolution panoramic photographs of the lunar surface. The areas photographed included the Hadley Rille landing sites (Figs. 4-1 and 4-2), several areas being considered as the Apollo 17 landing site, the Apollo 15 lunar module ascent stage impact point, near-terminator areas, and other areas of general coverage. Anomalous operation of the velocity/altitude sensor (section 14.3.1) was indicated on the first panoramic camera pass on revolution 4 and subsequent passes; however, good photography was obtained over all critical areas.

The delay in lunar module jettison caused cancellation of photographic passes planned for revolutions 58 and 59. These passes were rescheduled for revolutions 60 and 63, but sidelay with adjacent areas photographed on revolutions 33 and 38 was decreased.

All imagery is of very high quality. Examination of the film shows that less than one percent of the total film exposed was seriously degraded by the velocity/altitude sensor malfunction. 5.12.2 Mapping Camera.

The mapping camera was carried aboard the Apollo 15 service module to obtain high-quality metric photographs of the lunar surface. Mapping camera operation was desired during all panoramic camera passes and on selected dark-side passes to assist in analysis of data from the laser altimeter. The camera functioned normally and, essentially, the entire area overflown in daylight was photographed. However, the laser altimeter failed (see the following section) and all scheduled dark-side mapping activities subsequent to revolution 38 were deleted. A problem with the mapping camera deployment mechanism was also experienced. The camera extension and retraction cycles varied from 2 to 4 minutes as compared to about 1 1/2 minutes required prior to flight. After the last deployment, the camera did not completely retract. This anomaly is discussed further in section 14.3.3.

The mapping camera was turned off during the panoramic camera pass over the landing site on revolution 50 in a test to determine if the velocity/altitude sensor anomaly might be related to the mapping camera operation. This resulted in a minor loss of coverage. Also, the photographic pass planned for revolution 58 was deferred until revolution 60 because of the delay in lunar module jettison. The consequence of this was a decrease in sidelay below the desired 55 percent.

Approximately 6 hours of mapping camera operating time remained at transearch injection. About 1 1/2 hours of this were expended photographing the receding moon, and 3 1/2 hours were used photographing selected star fields with the stellar camera

associated with the mapping camera.

Image quality is excellent throughout the entire sequence of 3400 frames. The entire portion of the lunar surface which was overflowed by Apollo 15 in daylight has been covered by excellent stereoscopic photography which is as well suited to detailed analysis and geologic interpretation as it is to mapping.

### 5.12.2 Laser Altimeter

The laser altimeter was flown to accurately measure lunar topographic elevations in support of mapping and panoramic camera photography, and inflight experiments. The altimeter was designed to supply a synchronized altitude measurement for each mapping camera exposure on light-side photography, and independent altitude measurements on the dark side to permit correlation of topographic profiles with gravity anomalies obtained from spacecraft tracking data.

Operation of the altimeter was nominal through revolution 24, but improper operation was noted on the next operation (revolution 27). The performance of the altimeter became progressively worse until, on revolution 38, the altimeter ceased to operate (sec. 14.3.2). Consequently, the altimeter was not operated on subsequent dark-side passes, although operation on lightside mapping camera passes was continued. On revolution 63, an attempt was made to revive the altimeter through a switching operation by the Command Module Pilot, but the effort was not successful.

Approximately 50 percent of the planned altimeter telemetry data were actually obtained before the instrument failed. The data from the early orbits have been correlated with S-band transponder data for the frontside pass, and show the shape of the gravity anomalies as related to mare basins. The complete circumlunar laser altimeter data show that, relative to the mean lunar radius, the average lunar far side is about 2 kilometers (1.1 mile) high and the average near side is about 2 kilometers low.

### **5.13 COMMAND MODULE PHOTOGRAPHY**

While in lunar orbit, photographs were taken from the command module of lunar surface sites of scientific interest, and of specific portions of the lunar surface in earthshine and near the terminator. Also, while in lunar orbit, photographs were taken of low-light-level astronomical subjects including the solar corona, the zodiaca-1 light, lunar libration point L4, and of the moon as it entered and exited the earth's umbra during lunar eclipse. During translunar and transearth coast, photographs were taken of a contamination test and star fields were photographed through the command module sextant.

In accomplishing some of the tasks, the crewman obtained extra frames and some with longer exposures than required. This will enhance the value of the total data desired. The only 16-mm data acquisition camera magazine containing very-high-speed black-and-white film was lost. About 35 percent of the magazine had been exposed during lunar orbital flight and transearth coast for solar corona and sextant star field photography. The most probable cause of the loss of the magazine was that it floated through the hatch during the Command Module Pilot's extravehicular activity. This required a substitution of a slower black-and-white film magazine for the final sextant

star field photography and real-time update for contamination photography but, because premission-planned exposure settings were used with the much slower film, the sextant star field photographs are not clear.

Photographs were obtained of 21 of 23 specific lunar surface targets, the solar corona, the moon during lunar eclipse as it entered and exited the earth's umbra, star fields through the command module sextant, lunar libration region L4, and specific areas of the lunar surface in earthshine and in low light levels near the terminator. Near-terminator strip photography scheduled on revolution 58, and 2 of the 23 lunar surface targets scheduled on revolutions 58 and 59 were deleted because of the delay in lunar module jettison due to problems during tunnel venting operations and subsequent extension of the crew's sleep period. Based on preliminary examination of the dim-light photography, it appears that excellent quality imagery was obtained of the solar corona, the zodiacal light and the lunar surface in earthshine.

#### **5.14 VISUAL OBSERVATIONS FROM LUNAR ORBIT**

Visual observations from lunar orbit was an objective implemented for the first time on this mission. The Command module Pilot was asked to make and record observations of special lunar surface areas. Emphasis was to be placed on characteristics difficult to record on film, but which could be delineated by the eye, such as subtle color differences between surface units. All of the scheduled targets were observed and the results relayed. These results are documented in reference 2. Significant observations were as follows:

- a. Fields of cinder cones were discovered on the southeast rim of Mare Serenitatis (Littrow area) and the southwest rim of the same mare basin (Sulpicius; Gallos area).
- b. A landslide or rock glacier was delineated on the northwest rim of the crater Tsiolkovsky on the lunar farside (fig. 4-5).
- c. A ray-excluded zone around the crater Proclus on the west rim of Mare Crisium. was interpreted as being caused by the presence of a fault system at the west rim of the crater.
- d. Layers on the interior walls of several craters were found and were interpreted as volcanic collapse craters , or "caldera", in the maria.

## **6 COMMAND AND SERVICE MODULE PERFORMANCE.**

### **6.1 STRUCTURAL AND MECHANICAL SYSTEMS**

Command module accelerometer data indicated a sustained 5-hertz longitudinal oscillation of 0.35g peak-to-peak amplitude prior to first stage center engine cutoff. Similar oscillations have occurred on previous Apollo flights and are within acceptable structural design limits. Oscillations measured during second and third stage boost were less than 0.05g peak amplitude in any direction and were not structurally significant.

Translunar docking loads were higher than those of previous missions (see sec. 7-1).

Main parachute deployment for earth landing, beginning at approximately 10 500 feet, was normal. However, at approximately 6000 feet, one of the three main parachutes was observed to have collapsed. Details of this anomaly are reported in section 14.1.9.

### **6.2 ELECTRICAL POWER AND FUEL CELLS**

The electrical power system batteries and fuel cells performed satisfactorily throughout the mission.

The entry, auxiliary, and pyrotechnic batteries performed normally. Entry batteries A and B were charged nine times during flight (battery A - 4 times; battery B - 5 times). Load sharing and voltage delivery were satisfactory during each of the service propulsion firings. The batteries were near the fully charged level at entry.

The fuel cells were activated 59 hours prior to launch and the system was configured with fuel cell 2 on main bus A. Fuel cells 1 and 3 were on open-circuit until 3.5 hours before lift-off when fuel cells 1 and 2 were placed on main bus A and fuel cell 3 on main bus B. This configuration was maintained throughout the flight. Load variance between fuel cells was a nominal 4 to 7 amperes during flight, with the fuel cells supplying 653 kilowatt-hours of energy at an average current and bus voltage of 77 amperes and 28.8 volts, respectively.

### **6.3 CRYOGENIC STORAGE**

The cryogenic storage system satisfactorily supplied reactants to the fuel cells and metabolic oxygen to the environmental control system throughout the mission. The quantities of oxygen and hydrogen consumed as compared to preflight predictions are given in section 6.11-3.

The system supplied all demands including the extravehicular activity during transearth coast when the system supplied a flow rate of approximately 12.2 lb/hr and the pressure and heater temperatures remained within the anticipated limits.

## **6.4 COMMUNICATIONS**

Performance of the command and service module communications system was nominal throughout the mission, except that the Command Module Pilot's lightweight headset microphone was inoperative when the headset was removed from stowage. Inflight troubleshooting verified that the failure was in the microphone. Past history shows three microphone amplifier failures out of approximately 300 units in use. The headset was transferred to the lunar module and jettisoned; therefore, the failure could not be isolated to a specific component.

## **6.5 INSTRUMENTATION**

The instrumentation performed normally with three exceptions.

The service module reaction control system quad A fuel manifold pressure measurement was intermittently noisy (about 4 percent). However, there were other measurements for determining the manifold pressure.

The central timing equipment timer was reset at 97 hours 53 minutes. A time correction was inserted by up-data link, and the timer continued to operate properly throughout the flight. The noise susceptibility of the reset line to the central timing equipment has been evident on other spacecraft. However, because of the ease of updating, the problem has not been considered significant enough to justify redesign.

The first 20 feet of tape on the data recorder reproducer became degraded after about 100 dumps. This portion of the tape was not used for the remainder of the flight. This anomaly is discussed further in section 14.1.10.

## **6.6 GUIDANCE, NAVIGATION, AND CONTROL**

Performance of the guidance, navigation, and the primary and backup control systems was good throughout the flight. The two anomalies experienced during the mission were minor in nature causing no loss of system capability. They were excessive attenuation of light through the scanning telescope, and improper alignment of the roll axis when the gyro display alignment pushbutton was depressed. Descriptions of the anomalies and the corrective action being taken are included in sections 14.1.15 and 14.1.16.

The primary guidance system satisfactorily monitored the trajectories during launch and the translunar injection maneuver. The most probable velocity errors at insertion were minus 1.5, minus 41.5, and minus 10.8 ft/sec in the X, Y, and Z platform axes, respectively. The errors were determined from data obtained from several sources: the Saturn guidance system, the command module guidance system, the Saturn guidance system data modified by tracking data, and command module platform realignments in earth orbit.

Separation from the S-IVB and the transposition maneuver were nominal. During the

docking sequence, the digital autopilot control mode was changed from "attitude hold" to "free" while a plus-X translation was being commanded in order to secure a positive capture latch indication. The body rates induced by contact and the plus-X thrusting were not nulled and resulted in misalignment angles of minus 1-1.0, plus 2.2, and plus 1.6 degrees in pitch, yaw and roll at the start of the retract sequence (see fig. 6-1). The resultant misalignment caused a greater-than-normal structural loading in the docking interface (see sec. 7.1).

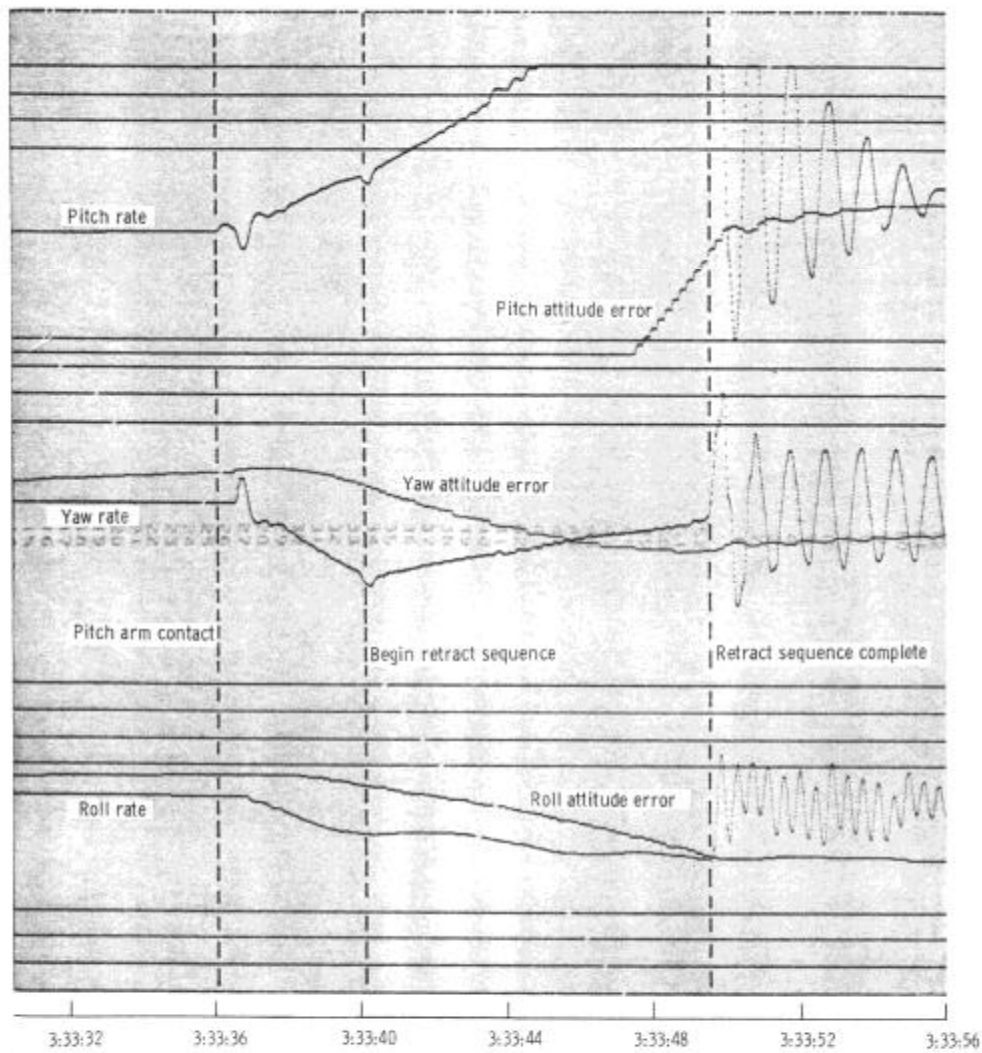


Figure 6-1. - Rate and attitude error data during transposition and docking sequence,

**Figure 6-1 - Rate and attitude error data during transposition and docking sequence.**

Body rate transients of less than 0.1 deg/sec in all three axes were caused by jettisoning of the scientific instrument module door and launching of the subsatellite.

Accelerometer biases and gyro drift terms were stable throughout the flight. The gyro drift terms were updated only once, at 27:56. **Table 6-I** is a summary of preflight histories and inflight performance data of the inertial components. **Table 6-II** is a summary of inertial measurement unit realignments performed during the mission. **Table 6-III** summarizes significant control parameters for each of the service propulsion system maneuvers.

TABLE 6-I.- INERTIAL COMPONENT CALIBRATION DATA

Parameter	Sample mean	Standard deviation	No. of samples	Countdown value	Flight load	Inflight Performance
Accelerometers						
X - Scale factor error, ppm . . . . .	-412	36	6	-489	-430	—
Bias, cm/sec <sup>2</sup> . . . . .	0.83	0.05	6	0.77	0.86	+0.90
Y - Scale factor error, ppm . . . . .	-170	25	6	-199	-200	—
Bias, cm/sec <sup>2</sup> . . . . .	-0.09	0.03	6	-0.10	-0.09	-0.05
Z - Scale factor error, ppm . . . . .	-165	48	6	-174	-180	—
Bias, cm/sec <sup>2</sup> . . . . .	-0.27	0.09	6	-0.25	-0.24	-0.20
Gyroscopes						
X - Null bias drift, meru . . . . .	1.42	0.96	10	1.80	2.0	+0.1
Acceleration drift, spin reference axis, meru/g . . . . .	-7.80	1.22	6	-7.0	-7.0	—
Acceleration drift, input axis, meru/g . . . . .	-10.25	2.44	6	-8.8	-12.0	—
Y - Null bias drift, meru . . . . .	-2.53	1.46	6	-3.2	-2.8	+0.1
Acceleration drift, spin reference axis, meru/g . . . . .	14.95	0.80	6	14.8	15.0	—
Acceleration drift, input axis, meru/g . . . . .	-2.0	3.78	12	-6.8	-5.0	—
Z - Null bias drift, meru . . . . .	-4.47	0.38	6	-5.0	-4.6	+0.1
Acceleration drift, spin reference axis, meru/g . . . . .	-2.45	0.76	6	-1.9	-2.0	—
Acceleration drift, input axis, meru/g . . . . .	0	1.03	6	1.5	0	—

TABLE 6-II.- COMMAND AND SERVICE MODULE PLATFORM ALIGNMENT SUMMARY

Time, hr:min	Program option*	Star used	Gyro torquing angle, deg			Star angle difference, deg	Gyro drift, sec			Comments
			X	Y	Z		X	Y	Z	
00:50	3	33 Antares, 41 Dabih	-0.029	+0.021	-0.061	0.01	-1.5	+1.7	+4.9	Launch orientation
5:30	3	01 Alpheratz, 07 Menkar	-0.102	-0.063	+0.166	0.01	+1.5	+0.9	+2.1	Launch orientation
5:33	1	01 Alpheratz, 07 Menkar	-0.731	+0.431	+0.315	0.01	—	—	—	Passive thermal control orientation
11:15	3	14 Canopus, 04 Achernar	-0.096	-0.088	+0.181	0.00	+1.1	+1.1	+2.1	Passive thermal control orientation
27:24	3	01 Alpheratz, 10 Mirfak	-0.329	-0.296	+0.576	0.00	+1.35	+1.1	+2.4	Passive thermal control orientation
55:21	3	10 Mirfak, 20 Deneb	-0.021	-0.034	-0.016	0.01	+0.1	+0.1	+0.0	Passive thermal control orientation
72:53	3	10 Mirfak, 20 Deneb	+0.012	-0.051	+0.015	0.00	+0.1	+0.2	+0.1	Passive thermal control orientation
75:15	3	36 Vega, 44 Enif	+0.025	+0.011	+0.001	0.00	-0.7	+0.3	+0.3	Passive thermal control orientation
75:19	1	36 Vega, 44 Enif	-0.363	+0.601	+0.263	0.00	—	—	—	Lunar orbit insertion orientation
80:04	3	40 Altair, 42 Peacock	-0.018	-0.006	-0.004	0.00	+0.3	+0.1	-0.1	Lunar orbit insertion orientation
80:10	1	37 Wukal, 45 Fomalhaut	+0.738	+0.898	+0.497	0.00	—	—	—	Landing site orientation
82:04	3	02 Diphda, 41 Dabih	-0.009	-0.007	+0.000	0.00	-0.3	+0.2	0.0	Landing site orientation
83:56	3	37 Wukal, 42 Peacock	+0.005	+0.004	+0.002	0.00	-0.2	-0.1	-0.1	Landing site orientation
95:43	3	25 Acrux, 26 Spica	+0.022	-0.032	+0.038	0.01	-0.1	+0.2	+0.2	Landing site orientation
97:39	3	41 Dabih, 42 Peacock	+0.010	-0.009	-0.025	0.01	-0.4	+0.3	-0.2	Landing site orientation
103:01	3	01 Alpheratz, 44 Enif	+0.023	-0.005	+0.009	0.00	+0.3	+0.1	+0.1	Landing site orientation
105:12	3	34 Atria, 45 Fomalhaut	+0.012	-0.011	+0.023	0.01	-0.2	+0.1	+0.3	Landing site orientation
109:07	3	04 Achernar, 42 Peacock	+0.015	-0.004	-0.014	0.00	+0.1	+0.1	-0.2	Landing site orientation
119:05	2	01 Alpheratz, 36 Vega	-0.028	-0.058	+0.012	0.01	+0.2	+0.4	+0.1	Landing site orientation
126:43	3	02 Diphda, 04 Achernar	+0.050	-0.007	+0.017	0.01	-0.4	+0.1	+0.1	Landing site orientation
130:38	3	02 Diphda, 04 Achernar	+0.016	-0.005	-0.017	0.01	-0.3	+0.1	-0.3	Landing site orientation
140:49	3	01 Alpheratz, 36 Vega	-0.004	-0.050	+0.041	0.01	0.0	+0.3	+0.3	Landing site orientation
152:46	3	41 Dabih, 43 Deneb	+0.028	-0.031	0.000	0.01	-0.2	+0.2	0.0	Landing site orientation
162:19	3	01 Alpheratz, 05 Polaris	-0.014	-0.044	+0.016	0.02	+0.1	+0.3	+0.1	Landing site orientation
164:18	3	41 Dabih, 43 Deneb	+0.050	-0.017	+0.005	0.01	-0.2	+0.1	0.0	Landing site orientation
164:22	1	41 Dabih, 43 Deneb	-0.641	+0.186	-0.042	0.00	—	—	—	Phase change orientation
166:09	1	41 Dabih, 43 Deneb	+0.125	-0.810	-0.730	0.00	—	—	—	Lunar orbit orientation
170:06	3	01 Alpheratz, 44 Enif	-0.006	-0.017	-0.017	0.00	+0.1	-0.3	-0.3	Lunar orbit orientation
193:52	3	06 Acamar, 45 Fomalhaut	+0.018	-0.081	-0.003	0.02	-0.1	+0.2	0.0	Lunar orbit orientation
202:00	3	01 Alpheratz, 40 Altair	+0.007	-0.047	-0.005	0.01	-0.1	+0.4	0.0	Lunar orbit orientation
211:52	3	34 Atria, 45 Fomalhaut	+0.029	-0.025	+0.018	0.01	-0.2	+0.2	+0.1	Lunar orbit orientation
219:28	3	06 Acamar, 45 Fomalhaut	+0.018	-0.027	-0.009	0.01	-0.2	+0.2	-0.1	Lunar orbit orientation
219:31	1	06 Acamar, 45 Fomalhaut	-0.474	+0.308	+0.433	0.00	—	—	—	Transearth injection orientation
221:27	3	03 Navi, 11 Aldebaran	+0.021	+0.004	+0.024	0.01	-0.7	-0.1	+0.8	Transearth injection orientation
226:11	3	11 Aldebaran, 16 Procyon	-0.015	-0.027	+0.004	0.00	+0.2	+0.4	+0.1	Transearth injection orientation
226:14	1	11 Aldebaran, 16 Procyon	+0.440	-0.522	+0.180	0.02	—	—	—	Passive thermal control orientation
236:25	3	31 Arcturus, 33 Antares	+0.019	-0.031	+0.027	0.02	-0.1	+0.2	+0.2	Passive thermal control orientation
251:00	3	41 Dabih, 43 Deneb	-0.008	-0.067	+0.034	0.00	0.0	+0.3	+0.2	Passive thermal control orientation
262:57	3	30 Menkent, 43 Alphecca	-0.017	-0.074	-0.021	0.00	0.0	+0.2	-0.1	Passive thermal control orientation
267:36	3	05 Polaris, 11 Aldebaran	-0.005	-0.006	+0.019	0.00	+0.1	+0.1	+0.3	Passive thermal control orientation
271:55	3	23 Denebola, 32 Alphecca	+0.029	-0.018	+0.001	0.01	-0.4	+0.3	0.0	Passive thermal control orientation
288:58	3	41 Dabih, 43 Deneb	-0.020	-0.087	+0.055	0.00	+0.1	+0.3	+0.2	Passive thermal control orientation
291:01	3	01 Alpheratz, 10 Mirfak	-0.016	-0.019	-0.003	0.00	+0.05	+0.6	-0.1	Passive thermal control orientation
293:21	1	01 Alpheratz, 10 Mirfak	-0.776	+0.175	+0.563	0.00	—	—	—	Entry orientation
293:21	3	40 Altair, 45 Fomalhaut	+0.006	-0.010	+0.005	0.01	-0.2	+0.3	+0.1	Entry orientation

\*1 - Preferred; 2 - Nominal; 3- REF3MMAT; 4 - Landing site.

TABLE 6-III.- GUIDANCE AND CONTROL MANEUVER SUMMARY

0-0

Parameter	Maneuver									
	First microse correction	Second microse correction	Lunar orbit insertion	Descent orbit insertion	Descent orbit split	Lunar orbit circulation	Lunar orbit plane change	Orbital swaying	Transmitta injection	Third microse correction
Time										
Ignition, hr:min:sec	22:46:00.00	23:31:34.81	28:31:46.70	87:39:49.09	95:56:44.70	101:36:58.98	145:11:32.75	221:20:48.02	229:58:45.06	291:56:49.91
Cutoff, hr:min:sec	22:46:07.80	23:31:25.77	28:31:25.06	87:40:13.62	95:57:15.10	101:39:02.45	145:11:31.05	221:20:34.44	229:58:16.74	291:57:17.21
Duration, min:sec	00:00.80	00:00.92	00:00.36	00:00.53	00:00.40	00:02.47	00:00.30	00:01.42	01:00.68	00:07.30
Velocity gained, ft/sec <sup>a</sup> (actual/desired)										
X	$\pm 5.5/M/A$	$\pm 3.2/\pm 3.2$	$\pm 1468.97/\pm 1468.9$	$\pm 195.57/\pm 196.1$	$\pm 2.8/\pm 2.1$	$\pm 748.3^c$	$\pm 59.8/\pm 59.4$	$\pm 62.9/\pm 62.9$	$\pm 2076.17/\pm 2069.6$	$\pm 2.3/\pm 2.8$
Y	$\pm 0.2/M/A$	$\pm 2.9/\pm 3.1$	$\pm 1749.3/\pm 1749.5$	$\pm 64.3/\pm 64.4$	$\pm 1.3/\pm 1.3$	$\pm 7.0^c$	$\pm 22.4/\pm 22.5$	$\pm 0.5/\pm 0.6$	$\pm 116.8/\pm 116.4$	$\pm 5.5/\pm 6.0$
Z	$\pm 0.1/M/A$	$\pm 3.0/\pm 3.0$	$\pm 2298.1/\pm 2298.1$	$\pm 56.17/\pm 56.2$	$\pm 0.3/\pm 0.1$	$\pm 7.0^c$	$\pm 228.3/\pm 228.2$	$\pm 21.1/\pm 21.4$	$\pm 939.13/\pm 939.4$	$\pm 2.27/\pm 1.1$
Velocity residual, ft/sec <sup>b</sup>										
X	N/A	$\pm 0.2$	0	$\pm 0.6$	$\pm 0.1$	0	0	$\pm 0.3$	$\pm 0.2$	$\pm 0.1$
Y		$\pm 0.1$	0	0	$\pm 0.2$	0	$\pm 0.4$	$\pm 0.7$	$\pm 0.6$	0
Z		$\pm 0.1$	0	$\pm 0.1$	$\pm 0.2$	$\pm 0.5$	$\pm 0.4$	$\pm 0.4$	$\pm 0.2$	$\pm 0.1$
Entry monitor system		$\pm 0.5$	$\pm 1.2$	$\pm 0.3$	$\pm 0.7$	$\pm 0.3$	$\pm 0.8$	$\pm 0.3$	$\pm 1.6$	$\pm 0.7$
Engine gimbal position, deg										
Initial										
Fitch	$\pm 1.36$	$\pm 1.25$	$\pm 1.23$	$\pm 1.72$			$\pm 0.36$	$\pm 0.63$	$\pm 0.59$	
Yaw	$\pm 0.23$	$\pm 0.33$	$\pm 0.56$	$\pm 0.49$			$\pm 1.04$	$\pm 0.95$	$\pm 0.82$	
Maximum excursion										
Fitch	$\pm 0.32$	$\pm 0.32$	$\pm 0.35$	$\pm 0.21$			$\pm 1.89$	$\pm 1.90$	$\pm 0.03$	
Yaw	$\pm 0.47$	$\pm 0.33$	$\pm 0.46$	$\pm 0.30$			$\pm 1.84$	$\pm 0.93$	$\pm 2.17$	
Steady-state										
Fitch	N/A	N/A	$\pm 1.39$	$\pm 1.84$			$\pm 1.04$	N/A	$\pm 0.72$	
Yaw	N/A	N/A	$\pm 0.05$	$\pm 0.44$			$\pm 0.95$		$\pm 0.34$	
Cutoff										
Fitch	$\pm 1.52$	$\pm 1.43$	$\pm 1.54$	$\pm 1.88$			$\pm 0.74$	$\pm 0.76$	$\pm 0.75$	
Yaw	$\pm 0.77$	$\pm 0.67$	$\pm 0.64$	$\pm 0.49$			$\pm 0.91$	$\pm 0.40$	$\pm 0.40$	
Maximum rate excursion, deg/sec										
Fitch	0	0	$\pm 0.11$	$\pm 0.19$			$\pm 1.06$	$\pm 1.06$	$\pm 0.64$	
Yaw	$\pm 0.19$	$\pm 0.17$	$\pm 0.21$	$\pm 0.25$			$\pm 1.09$	$\pm 0.99$	$\pm 1.67$	
Roll	$\pm 0.12$	$\pm 0.08$	$\pm 0.18$	$\pm 0.35$			$\pm 1.85$	$\pm 1.17$	$\pm 1.58$	
Maximum attitude error, deg										
Fitch	0	0	$\pm 0.22$	$\pm 0.37$			$\pm 0.37$	$\pm 0.18$	$\pm 0.20$	
Yaw	$\pm 0.08$	0	$\pm 0.18$	$\pm 0.21$			$\pm 0.27$	$\pm 0.33$	$\pm 0.25$	
Roll	0	0	$\pm 5.00$	$\pm 0.26$			$\pm 0.90$	$\pm 0.99$	$\pm 3.00$	

<sup>a</sup>Inertial coordinates.  
<sup>b</sup>Body coordinates.  
<sup>c</sup>From noseless pad in local vertical coordinates.  
<sup>d</sup>Plus sign indicates less than desired velocity.

During lunar orbital operations between 84 and 95 hours , the command and service module maintained a period of local horizontal attitude hold with the scientific instrument module toward the lunar surface. The evaporator in the primary coolant loop was turned off to prevent interference with the inflight science activities. The resulting large temperature oscillations in the coolant loop gave some concern as to how these temperature excursions would affect the guidance equipment. Since no direct guidance equipment telemetry measurements of coolant temperatures were available, an analysis was performed using a thermal model of the coolant loop and a ground test was performed with non-flight guidance equipment. Both indicated that considerable temperature attenuation exists in the coolant loop and that temperatures experienced during the flight were within acceptable limits. As a result of the thermal analysis, the maximum temperature limits in the systems operational data book are being raised to 90 F, peak, and 75 F, average, over a 2-hour period. The effect of coolant temperature oscillations upon accelerometer bias is shown in **Figure 6-2**.

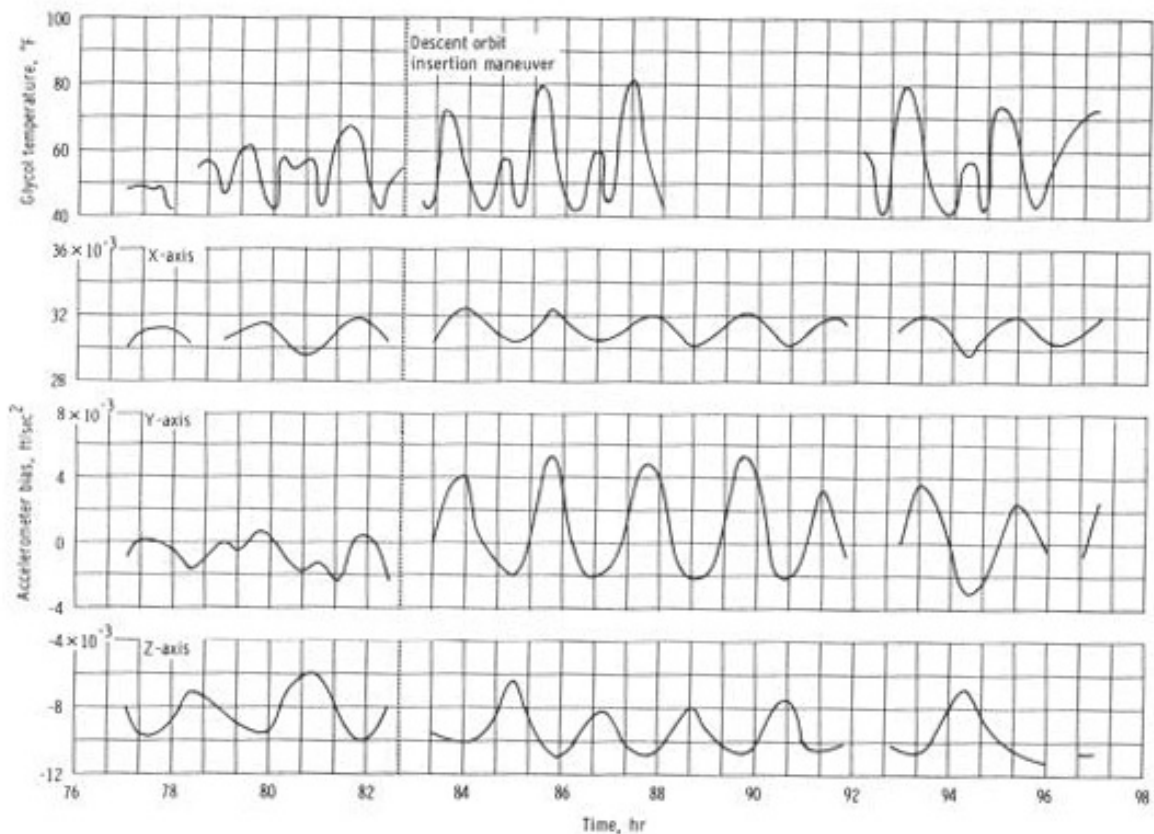


Figure 6-2.- Effect of coolant temperature oscillations on accelerometer bias during lunar orbit.

Cislunar midcourse navigation exercises were performed during the transearth phase to again demonstrate the capability to navigate to safe entry conditions in the absence of communications with earth.

Separation from the service module, the maneuver to entry attitude, and sensing of 0.05g during entry were all nominal. The command module dynamics were seen to change suddenly when the parachute failure resulted in a decrease in lift (sec. 14.1.9).

The guidance system controlled the vehicle attitude and lift vector during entry and, based on computer readouts, guided the spacecraft to landing coordinates of 26 degrees 7 minutes 48 seconds north latitude, and 158 degrees 7 minutes 12 seconds west longitude.

Postflight testing of the entry monitor system scroll indicated that intermittent scribing occurred after drogue deployment. Chemical analysis revealed an improper mixture of the phenolic resin and the encapsulated dye which is used to coat the scroll. The trace

that was scribed by the stylus was visible to the crew during entry but was not visible postflight because the dye and resin did not develop properly. No hardware changes will be made since only postflight testing of the scroll is affected.

## **6.7 PROPULSION**

### 6.7.1 Reaction Control Systems

Performance of the service module reaction control system was normal throughout the mission except that some service module propellant isolation valves closed as on previous missions. Indications that valves were closed were reported by the crew following launch, S-IVB/command and service module separation, and scientific instrument module door jettison. In all cases, the valves were recycled open without incident. A more complete discussion of this anomaly is given in section 14.1.1.

The performance of the command module reaction control system was nominal throughout the mission. The effects of dumping raw fuel following the propellant depletion firing sequence and the association of this procedure with the parachute failure is discussed in section 14.1.9.

### 6.7.2 Service Propulsion System

Service propulsion system performance was satisfactory during each of the eight maneuvers. The steady-state pressure data, gaging system data, and velocity differentials indicated essentially nominal performance. Engine ignition procedures for lunar orbit insertion and transearth injection were revised, however, because of a short which developed in the ignition control circuitry on the downstream side of the bank A solenoid valve. A discussion of this malfunction is given in section 14.1-3.

Previous flight results have shown the inflight mixture ratio to be significantly less than expected from engine acceptance test data. The service propulsion system engine was re-orificed to increase the mixture ratio for this mission. **Figure 6-3** shows the propellant unbalance for the two major engine firings compared with the predicted unbalance. The unbalance at the end of the transearth injection firing was very small and shows that the modifications to the engine were satisfactory.

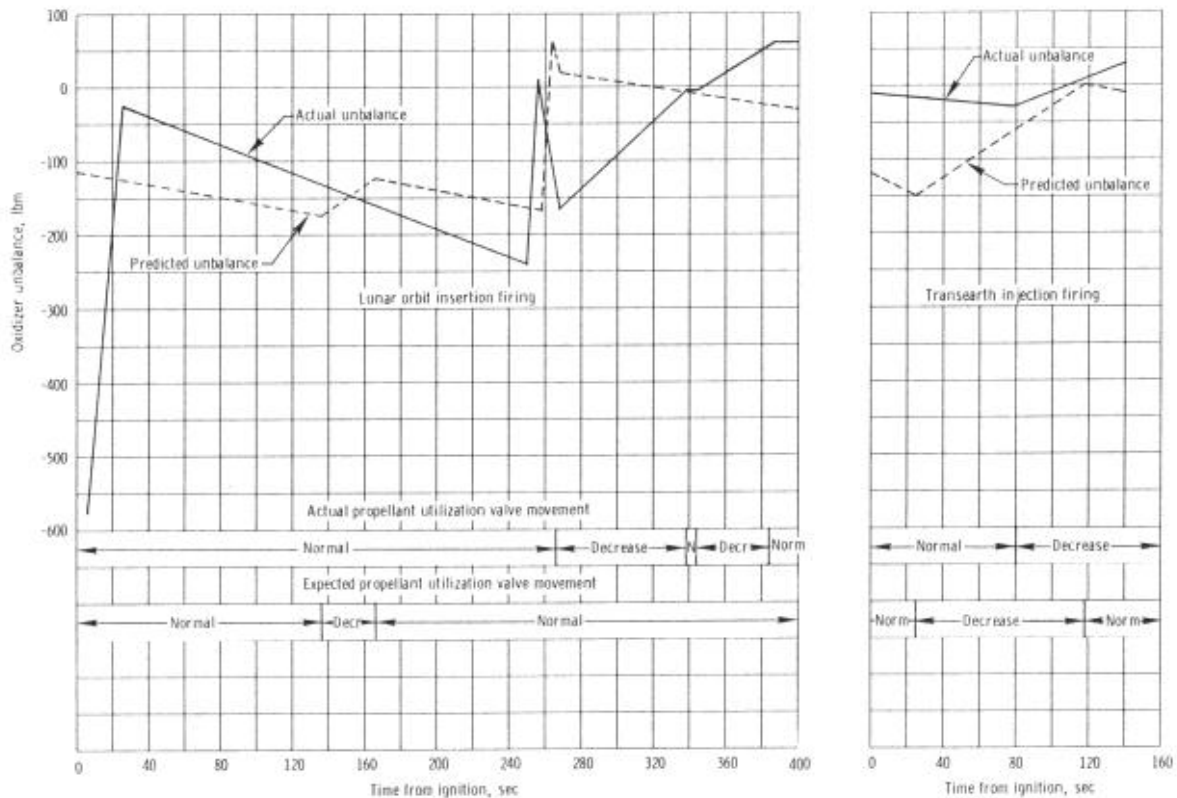


Figure 6-3.- Propellant unbalance during the lunar orbit insertion and transearth injection firings.

## 6.8 ENVIRONMENTAL CONTROL AND CREW STATION

### 6.8.1 Environmental Control System

Performance of the environmental control system was satisfactory, although several discrepancies required corrective action or minor changes to the planned operations.

Water leakage at the chlorine injection port was noted on two occasions when the cap was removed for the daily chlorination. Retightening of the port septum-retention insert by the crew successfully stopped the leakage (see sec. 14.1.2). The crew also noted the presence of gas in the water, especially after heavy usage such as at the end of an eating period (see sec. 14.1.14). Another problem related to drinking water was that, on two occasions, at 13 1/2 hours and 277 hours, the potable water tank failed to refill after use while the waste water tank accepted the normal fuel cell water production. Proper potable tank filling resumed after a waste water dump at 28 1/2 hours, but the tank failed to refill after meal preparation at 277 hours (see sec. 14.1-7).

Command module cabin pressure was increased prior to sleep periods again on this flight to assist in measuring inflight cabin leakage. Estimates of 0.03 lb/hr during translunar coast and 0.01 lb/hr during transearth coast were determined from cabin pressure decay data.

Noises were heard from the cabin fans that were believed to have been caused by an object striking the fan blades. Cycling of the fans allowed the fans to run normally (see sec. 14.1.13).

Prior to crew transfer for lunar module housekeeping, difficulty was experienced in obtaining proper lunar module/command module differential pressure gage readings. The difficulty resulted in insufficient lunar module pressure decay at cabin pressure equalization. Consequently, extra lunar module venting was required to obtain additional oxygen enrichment and assure minimum oxygen concentration for later suited activities.

Radiator outlet temperatures while in translunar coast and lunar orbit. were 10 to 150 F higher than preflight thermal studies indicated they would be. During the flight, calculations using more accurate heat load inputs resulted in considerably closer predictions, although some degradation of radiator coating may have contributed to the higher-than-predicted temperatures. The radiator outlet temperatures were greater than on previous missions because of the vehicle attitude and higher electrical loads required to support the scientific instrument module experiments.

During preparations for lunar module jettison, after an apparently successful hatch integrity check, the differential pressure decreased between the command module cabin and tunnel, indicating the possibility of a command module hatch leak. Although a subsequent 10-minute check demonstrated satisfactory hatch integrity, an inspection of both the lunar module and command module hatch seals was made. No evidence of contamination or damage was found. The hatches were reinstalled and a successful hatch integrity check was performed. The crew had also experienced difficulty in obtaining an acceptable suit circuit integrity check during the lunar module jettison preparations. After being unable to pressurize the suit loop more than 1 psi above cabin pressure, the crew doffed their helmets and gloves, and the Commander also unzipped his pressure garment assembly, unlocked and removed the liquid cooling garment connector, and installed a water connector plug. After reziping the suit and donning helmets and gloves, a successful integrity check was completed. Subsequently, because of the hatch integrity problem previously mentioned, the suit integrity was again broken, and the suit check had to be repeated. This check was again unsatisfactory because one suit glove was not properly connected. After making the correct connection, a final suit circuit test was successfully completed. The delay resulted in the lunar module being jettisoned one revolution later than planned.

Droplets of water came from two of the three blue (supply) hoses when they were relocated for the transearth injection firing. Since cabin humidity continued to be normal and no recurrence of the problem was observed, most likely the condensation was an effect of the large primary coolant loop temperature transient on the suit circuit heat exchanger during lunar orbit.

During the period of the entry propellant depletion firing, cabin pressure continued to increase at a rate consistent with the ambient atmospheric entry pressure. Manual closure of the cabin pressure relief valves at that time should have prevented any additional inflow. Since use of onboard gas supplies was not sufficient to account for the change, apparently the manual valve was not completely closed or abnormally high

leakage occurred. Postflight examination of the cabin pressure relief valves and the remote operating mechanism was conducted, and no excess leakage was indicated.

While being used for postflight testing, the side-A shutoff valve on the main oxygen regulator toggle arm pivot pin was found sheared. No problem had been reported during the mission. This anomaly is discussed further in section 14.1.18.

### 6.8.2 Crew Station/Equipment

The performance of crew equipment was satisfactory. Three items of equipment were reviewed as a result of problems experienced during the mission.

The command module ultraviolet window filter was inspected to determine what action may be required to prevent surface scratching and improve the optical qualities of the filter. A change has been made to the filter material to improve the abrasive resistance and optical qualities.

Lengthening of the Command Module Pilot restraint tether was investigated to provide additional reach for the crewman. The current length is the maximum allowable to preclude loading of the oxygen umbilicals.

The command module crewman optical alignment sight which came loose from its mount during landing has been inspected. This anomaly and the corrective action being taken are discussed in section 14.1.19.

## 6.9 **CONTROLS AND DISPLAYS**

The controls and displays performed normally with the following exceptions.

Direct-current bus B and alternating-current bus 2 undervoltage alarms occurred at approximately 33-3/4 hours; subsequently, an integral lighting circuit breaker was found open. Since the circuits fed by this breaker were not mission essential, the breaker was not reset. See section 14.1.4 for further discussion of this anomaly.

At approximately 81-1/2 hours, the battery relay bus measurement read 13.66 volts instead of the nominal 32 volts, as evidenced by backup measurement readings. Movement of the panel 101 systems test meter switch caused the reading to return to normal. This anomaly is discussed in section 14.1.5.

The mission timer on panel 2 stopped at about 125 hours. After several attempts, the timer was restarted, and it operated properly for the remainder of the mission. See section 14.1.8 for further discussion of this anomaly.

During the crew debriefing, the Command Module Pilot stated that the seconds digit of the digital event timer located on panel 1 became obscured by a powder-like substance that formed on the inside of the glass. For further discussion, see section 14.1.11.

Another problem noted during postflight testing of the vehicle was that the battery charger main A circuit breaker on panel 5 could not be manually opened. Corrosion was

found around the indicator sleeve of the breaker actuating knob. This anomaly is discussed in section 14.1-17.

### **6.10 EXTRAVEHICULAR ACTIVITY EQUIPMENT**

The environmental control system and crew equipment performed successfully throughout the transearth extravehicular activity. Operation of the new components, including the umbilical, suit control unit, pressure control valve, oxygen control and communications panels, and the extravehicular activity warning system was entirely nominal. All checks and activities went smoothly, and the extravehicular portion lasted less than 40 minutes. Cabin pressure was restored as planned, using the three 1-pound oxygen bottles from the rapid repressurization system and CMP-flow mode until 3.0 psia was reached, and then discharging the unused oxygen purge system to bring the pressure above 5.0 psia. Subsequent depletion of the residual 2000 psi in the oxygen purge system was accomplished by using it once to increase cabin pressure prior to a sleep period and on the following day, when the remainder was allowed to bleed into the cabin at a controlled rate.

### **6.11 CONSUMABLES**

The command and service module consumable usage during the Apollo 15 mission was well within the red line limits and, in all systems, was close to the preflight predicted values.

#### **6.11.1 Service Propulsion Propellant**

Service propulsion propellant and helium loadings and consumption values are listed in the following table. The loadings were calculated from gaging system readings and measured densities prior to lift-off.

Condition	Propellant, lb		
	Fuel	Oxidizer	Total
Loaded	15 664.0	25 035.6	40 699.6
Consumed	14 965.0	23 918.6	38 883.6
Remaining at end of transearth injection	699	1117.0	1816.0
Usable at end of transearth injection	553	822.0	1375

Condition	Helium, lb	
	Storage Bottles	Propellant Tanks
Loaded	85.5	5.4
Consumed	65.6	-
Remaining at end of transearth injection	19.9	71.0

### 6.11.2 Reaction Control System Propellant

Service Module.- The propellant utilization and loading data for the service module reaction control system were as shown in the following table. Consumption was calculated from telemetered helium tank pressure histories and was based on pressure, volume, and temperature relationships.

•••••

Condition	Propellant, lb		
	Fuel	Oxidizer	Total
Loaded			
Quad A	109.3	225.8	335.1
Quad B	109.3	224.0	333.3
Quad C	109.7	224.5	334.2
Quad D	109.5	224.1	333.6
Total	437.8	898.4	1336.2
<sup>a</sup> Usable loaded			1214
Consumed			810
Remaining at command module/ service module separation			404

<sup>a</sup>Usable loaded propellant is the amount loaded minus the amount trapped with corrections made for gaging system errors.

Command Module.- The loading and utilization of command module reaction control system propellant were as follows. Consumption was calculated from pressure, volume, and temperature relationships.

Condition	Propellant, lb		
	Fuel	Oxidizer	Total
Loaded			
System 1	44.2	77.6	121.8
System 2	44.3	78.4	122.7
Total	88.5	156.0	244.5
<sup>a</sup> Usable loaded			208
<sup>b</sup> Consumed			
System 1			30
System 2			30
Total			60

<sup>a</sup>Usable loaded propellant is the amount loaded minus the amount trapped.

<sup>b</sup>Estimated by using pressure, volume, temperature, and engine firing time summation techniques.

### 6.11.3 Cryogenics

The total cryogenic hydrogen and oxygen quantities available at liftoff and consumed were as follows. Consumption values were based on quantity data transmitted by telemetry.

Condition	Hydrogen, lb		Oxygen, lb	
	Actual	Planned	Actual	Planned
Available at lift-off				
Tank 1	27.4		313	
Tank 2	26.7		316	
Tank 3	26.4		<sup>a</sup> 324	
Total	80.5	<sup>b</sup> 80.5	953	<sup>b</sup> 952
Consumed				
Tank 1	20.6		176	
Tank 2	20.7		180	
Tank 3	18.3		206	
Total	59.6	59.5	562	556
Remaining at command module/service mod- ule separation				
Tank 1	6.8	8.5	137	138
Tank 2	6.0	5.4	136	142
Tank 3	8.1	7.1	118	116
Total	20.9	21.0	391	396

<sup>a</sup>Moved off upper limits at 15 hours

<sup>b</sup>Updated to lift-off values

#### 6.11.4 Water

The water quantities loaded, produced, and expelled during the mission are shown in the following table.

Condition	Quantity, lb
Loaded (at lift-off)	
Potable tank	28.6
Waste tank	27.6
Produced inflight	
Fuel cells	520.5
Lithium hydroxide	26.7
Metabolic	26.0
Dumped overboard	
Waste tank	420.5
Potable tank	15.5
Urine and flushing	<sup>a</sup> 102.6
Evaporator usage	8.0
Water samples	1.5
Remaining at command module/ service module separation	
Potable tank	31.0
Waste tank	51.3

<sup>a</sup>This is the quantity required to complete the water balance. Standard Operations Data Book values based on an average metabolic rate of 467 Btu/hr per man indicate a urine and feces production of 87.3 lb. Water for flushing is estimated at 4.2 lb based on 50 cc per flush (40 urinations). The difference between these standard values and the quantity required to complete the balance is 11.1 lb and is considered as unresolved usage.

## 7 LUNAR MODULE PERFORMANCE

### 7.1 STRUCTURAL AND MECHANICAL SYSTEMS

The structural loads were within design values for all phases of the mission based on guidance and control data, cabin pressure measurements, command module acceleration data, photographs, and crew comments.

Translunar docking loads were higher than those of previous missions because of a pitch misalignment angle of 11 degrees between the command and service module and the lunar module/S-IVB prior to docking probe retraction to the hard-docked configuration. The bending moment during translunar docking was computed to be 425,000 inch-pounds which approaches the design limit of 437,000 inch-pounds.

The sequence films from the onboard camera showed no evidence of large structural oscillations during lunar touchdown, and crew comments agree with this assessment. Landing on the lunar surface occurred with estimated velocities of 6.8 ft/sec in the minus X direction, 1.2 ft/sec in the plus Y direction, and 0.6 ft/sec in the plus Z direction. The descent rate at probe contact was 0.5 ft/sec. Following probe contact, the descent engine was shut down while the footpads were still about 1.6 feet above the surface, resulting in the 6.8 ft/sec velocity at footpad contact. Computer simulations indicate 1.0 inch of stroke in each primary strut except the forward strut, for which a 3.0-inch stroke is estimated. The simulations also indicate that the forward footpad was off the surface in the final rest position. The crew stated that the forward footpad was loose and rotated easily, confirming the computer results.

At touchdown, the lunar module was located partially inside a small crater with the rim of the crater directly underneath the descent engine skirt. The descent engine skirt buckled during landing. This is accounted for in the touchdown dynamic analysis, and was expected as the skirt length had been extended 10 inches over that of previous vehicles. This buckling was noted by the crew and confirmed by photographs of the damaged skirt (**Fig. 7-1**).